Lecture 6: Geometric Modeling and Visualization

Boundary & Finite Element Meshed Models II: Contouring

Chandrajit Bajaj

http://www.cs.utexas.edu/~bajaj

Center for Computational Visualization
Institute of Computational and Engineering Sciences
Department of Computer Sciences
University of Texas at Austin

October 2007

Imaging2Models

1. X-ray Crystallography → 2D Image Processing → Atomic Centers/Bonds (PDB) → FCC → Surface, Volume Processing → BEM/FEM/Shells
2. Single Particle Cryo-EM → 2D Image Processing → 3D Reconstruction → 3D Image Processing → Symmetry, Surfaces, Volume Processing→ BEM/FEM/Shells
3. Single-section EM/Anisotropic CT/MRI -> 2D Image Processing -> Planar X-section Contour Stack -> BEM/FEM/Shells
4. Tomographic EM/MicroCT/CT/MRI → 3D Image Processing → Higher Order 3D Reconstructions, Surfaces, Skeletons → BEM/FEM/Shells
5. Time Dependent Mesh Maintenance

Contouring: Capturing the Topology and Geometry of Zero Sets

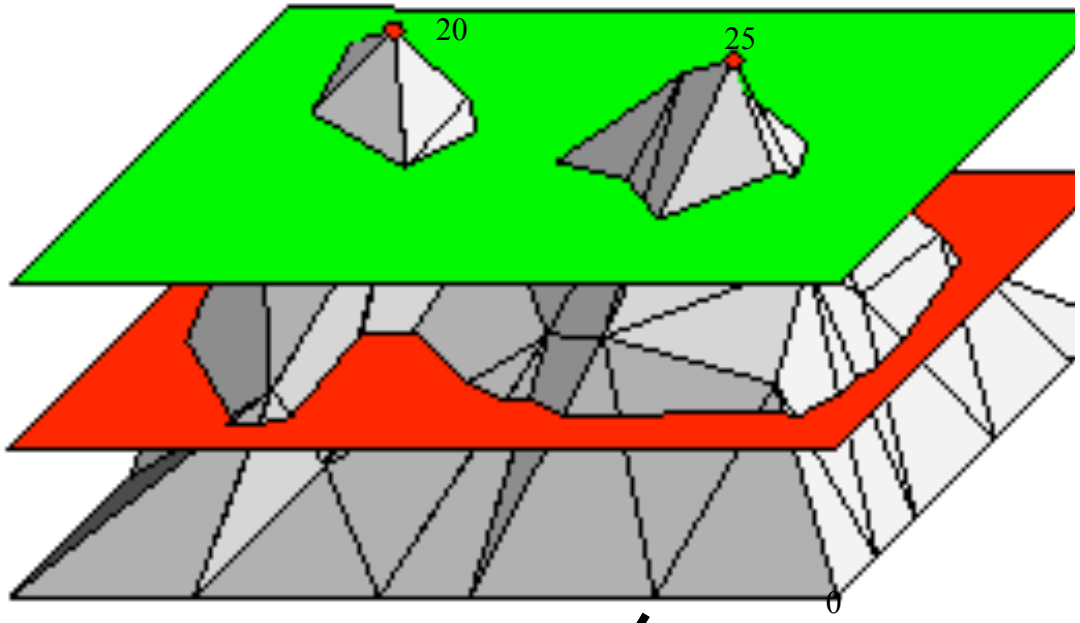

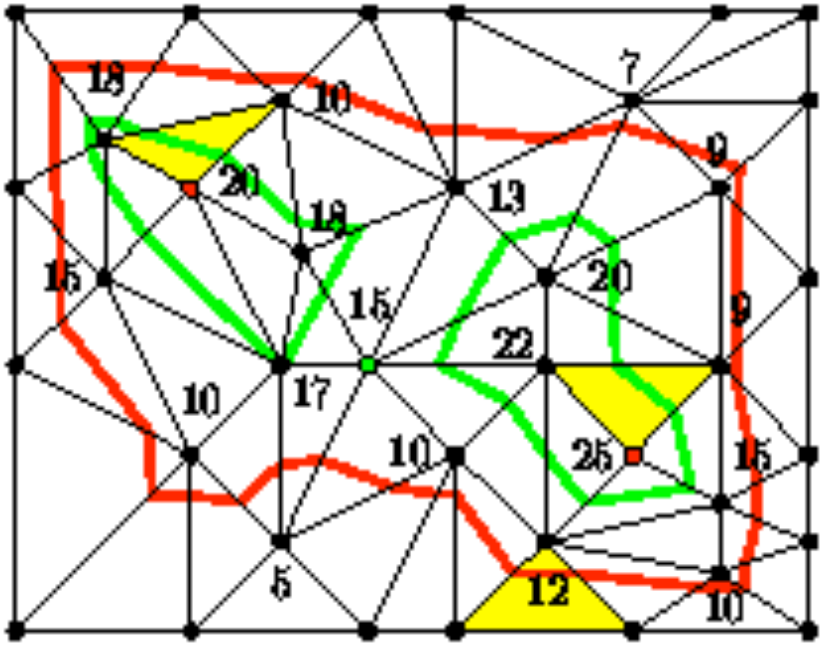

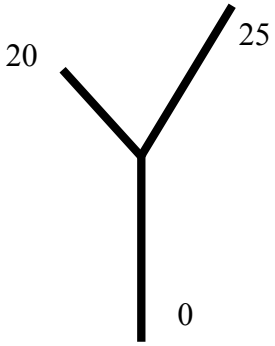

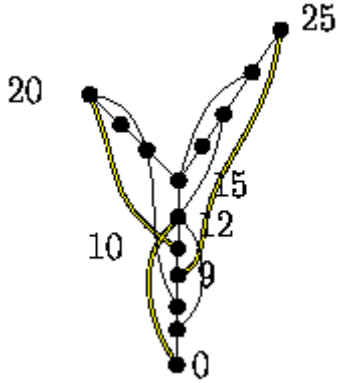

Acetylcholinesterase (AChE)

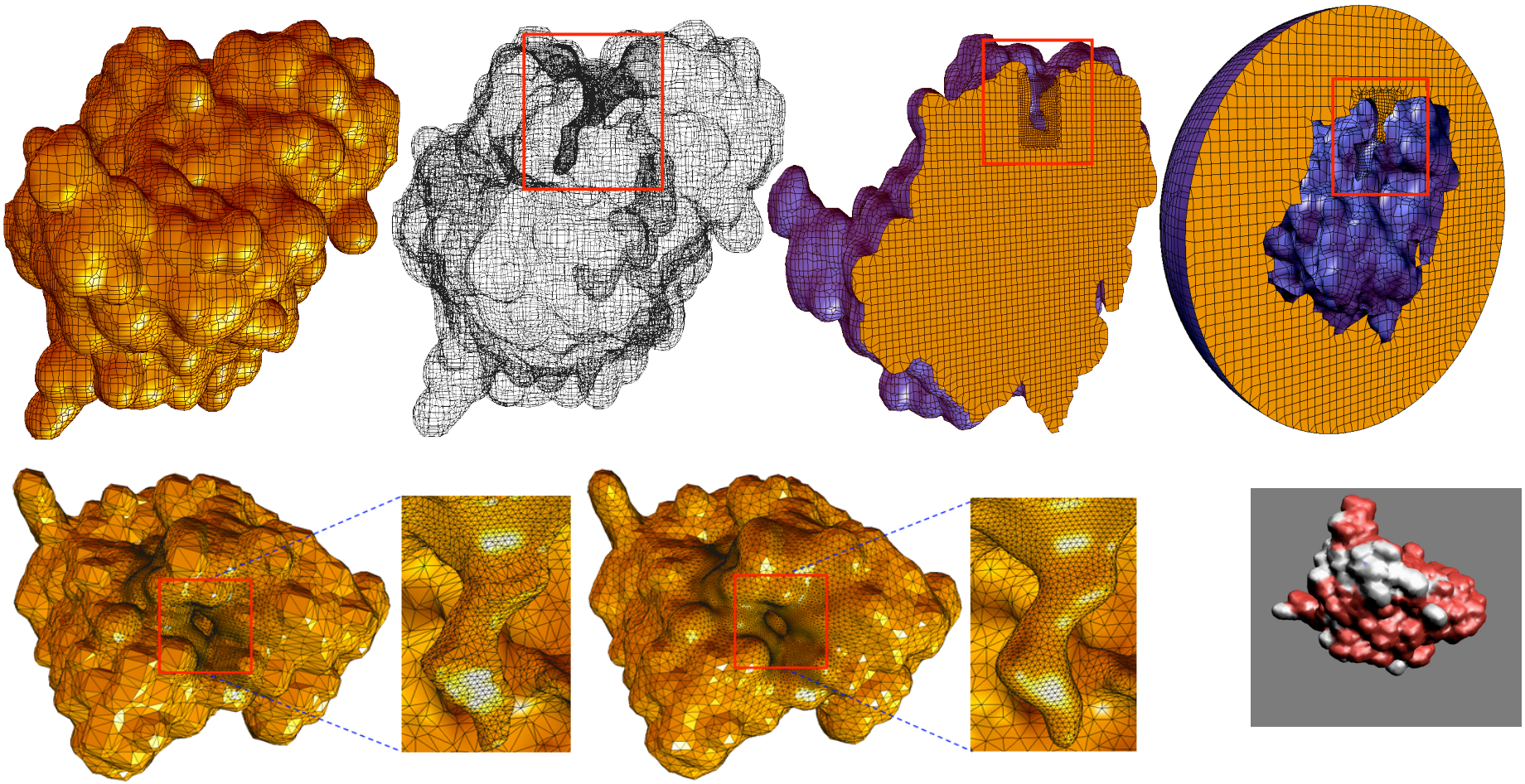

PB electrostatics potential calculation via APBS (Baker, Holst, McCammon)

Segmentation &Tetrahedral Meshing of the Synaptic Cleft Domain

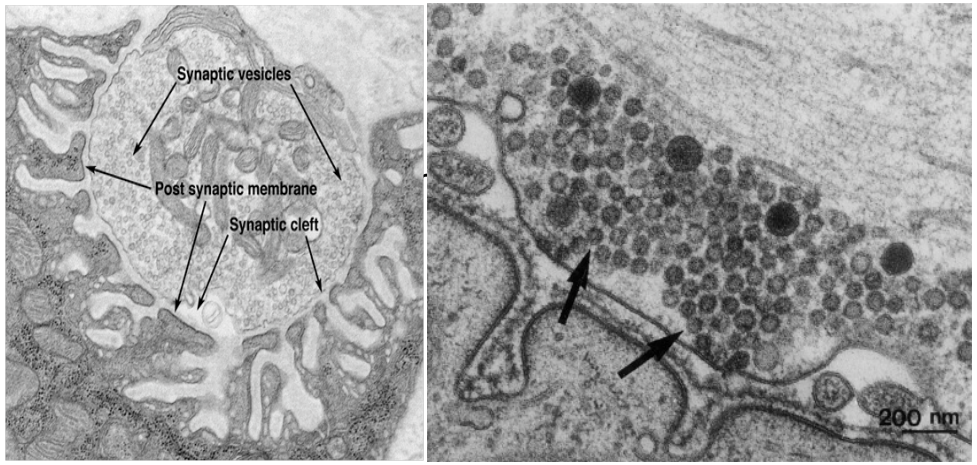

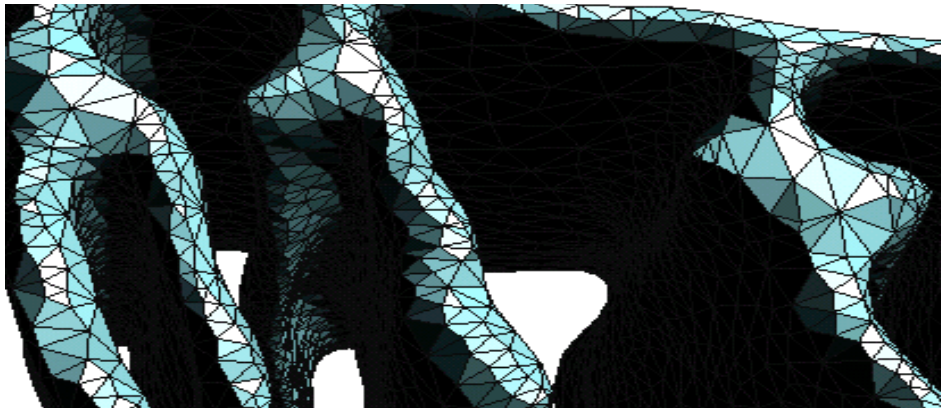

Segmented Triangular Mesh

Interior Tet Mesh (224475 vertices, 1077728 tetrahedra)

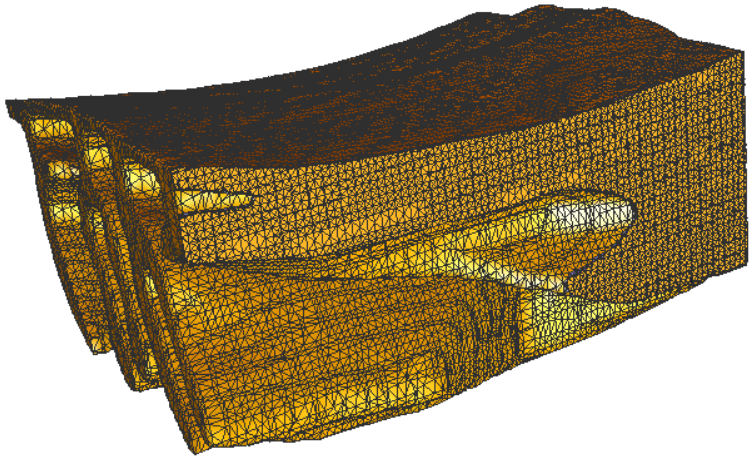

LBIE Mesher

Center for Computational Visualization
Institute of Computational and Engineering Sciences
Department of Computer Sciences
University of Texas at Austin

October 2007

Tet. Mesh of Segmented Rice Dwarf Virus Subunit via LBIE Mesher

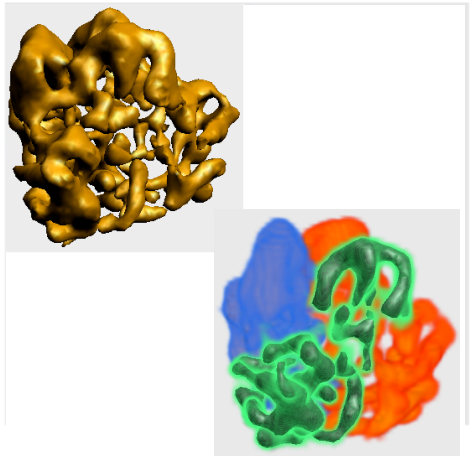

(a) segmented subunits

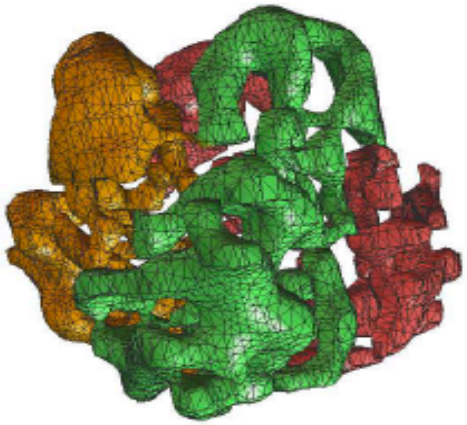

(b) side view

(c) cross section

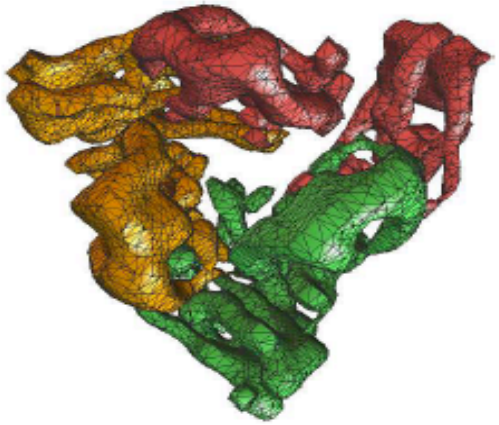

(d) top view

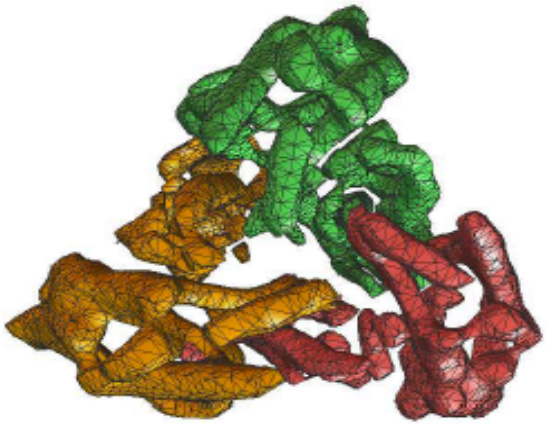

(e) bottom view

A-Patch Approximation

- ~9200 points, 406 patches (degree 3), 1% error

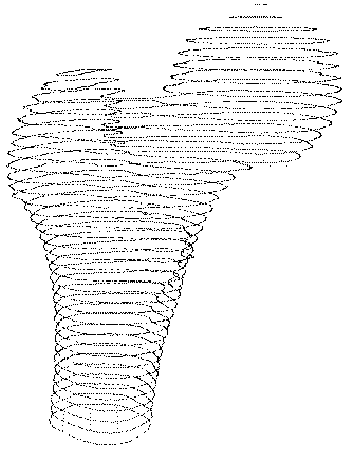

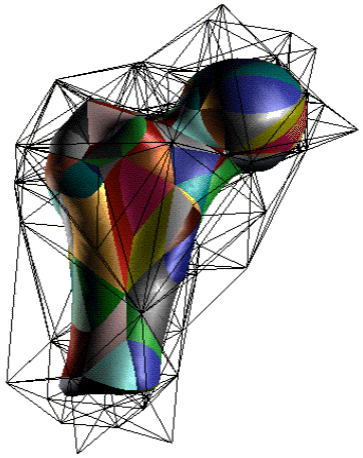

Modeling Human Joint Dynamics and Stress

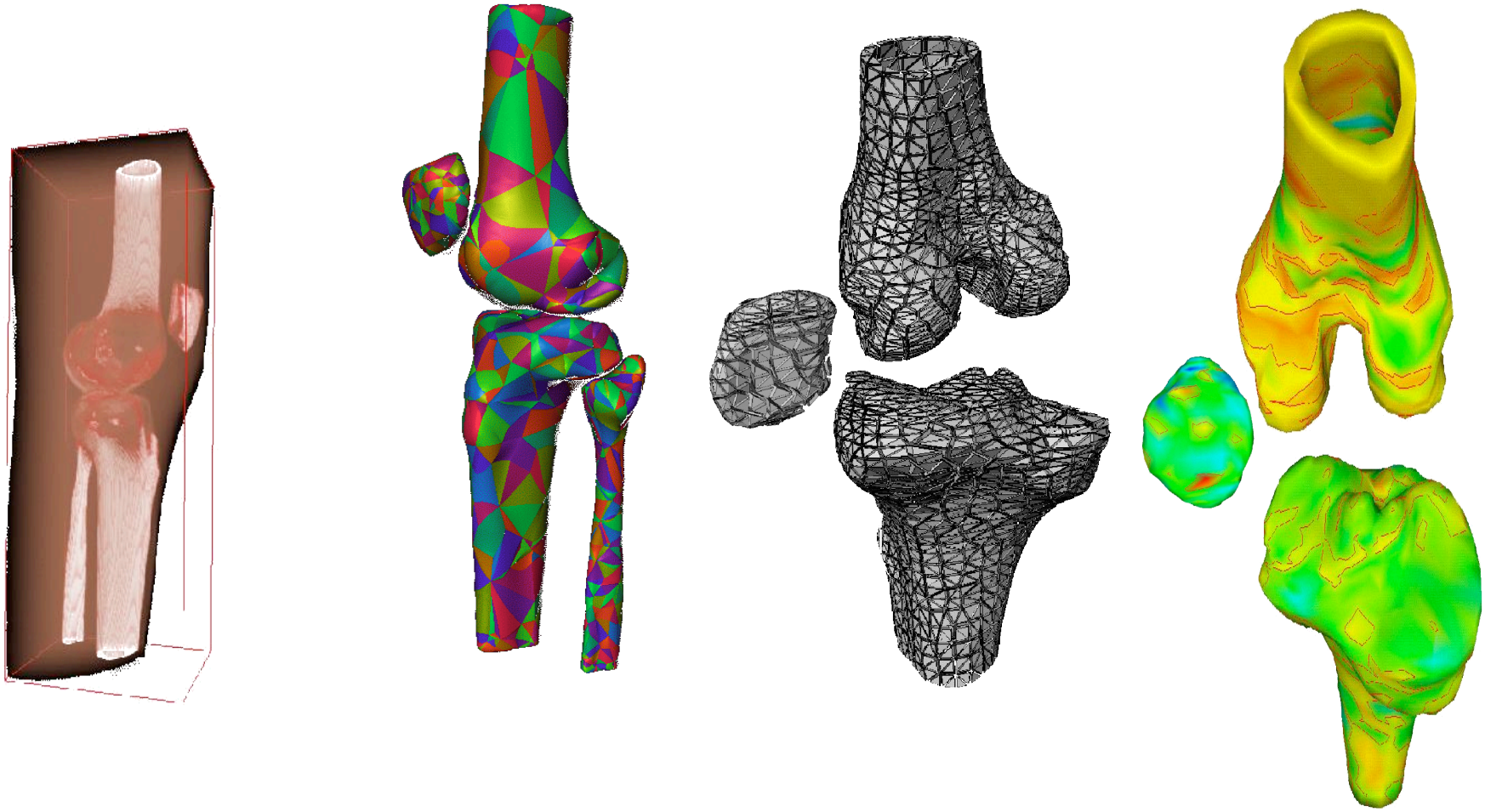

Tri/Tetra Meshing using Contouring

- Structured Meshing - All interior nodes have an equal number of adjacent elements, or the node valence is equal.
- Unstructured Meshing – the node valence is relaxed.
  - Octree technique – Shephard 1984, 1991.
    Input: a pre-defined surface mesh
    Method: recursively subdivide the cubes containing the geometric model until the desired resolution is reached, meshes are generated from the irregular boundary cells and regular interior cells.
  - Advancing front method – Lohner 1988, 1996; Lo 1991.
    Input: a pre-defined surface mesh
    Method: tetra are built progressively inward from the triangulated surface, an active front is maintained when new tetra are formed.
  - Delaunay – Delaunay 1934; Lawson 1977; Watson 1981; Weatherill 1994; Chew 1989; Ruppert 1992; Shewchuk 1996.
    Input: a set of vertices Delaunay criterion: “empty sphere”
    Method: nodes are triangulated according to the Delaunay criterion. New nodes are inserted, redefining the triangles or tetra locally to maintain the criterion. Different point insertion algorithms and guaranteed–quality mesh generation were studied by Weatherill, Chew, Ruppert, Shewchuk and etc.
  - Isosurface extraction from imaging data
    - Marching Cubes - Lorensen & Cline 1987, Fujishiro et. al. 1996.
    - Interval volume tetrahedralization – Nielson & Sung, 1997.
    - Dual Contouring – Ju et. al., 2002.

Tri/Tetra Meshing

- Dual Contouring of Hermite Data
  [Ju et al. 2002]

$$QEF[x] = \sum_i (n_i \cdot (x - p_i))^2$$

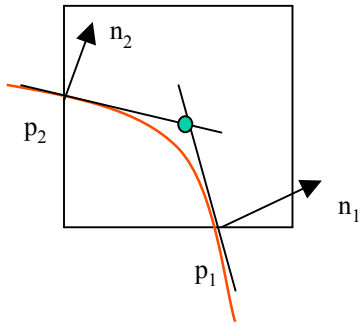

Boundary Intersection Edge - An edge whose one vertex lies inside the isocontour while the other vertex lies outside.

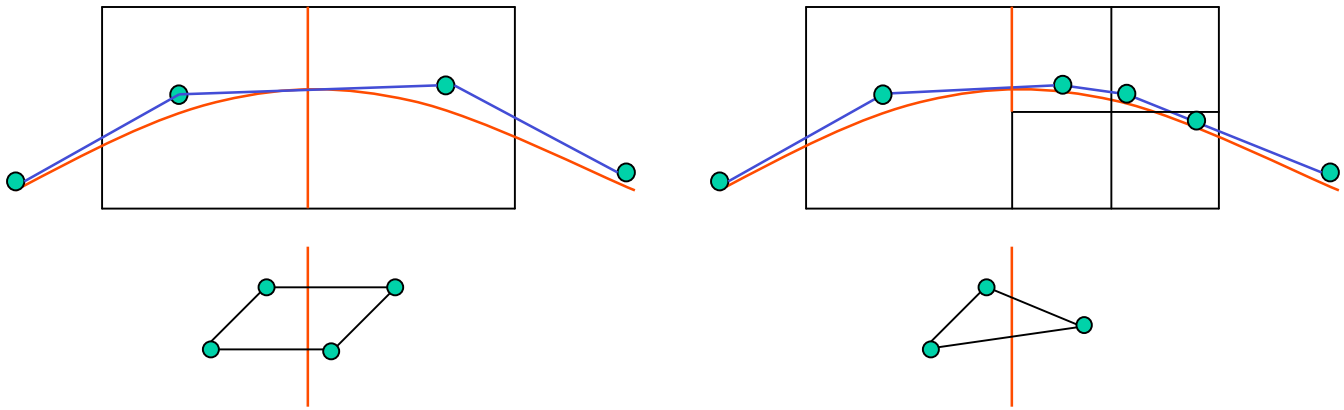

uniform

adaptive

Topology of Zero-Sets of a Tri-linear Function

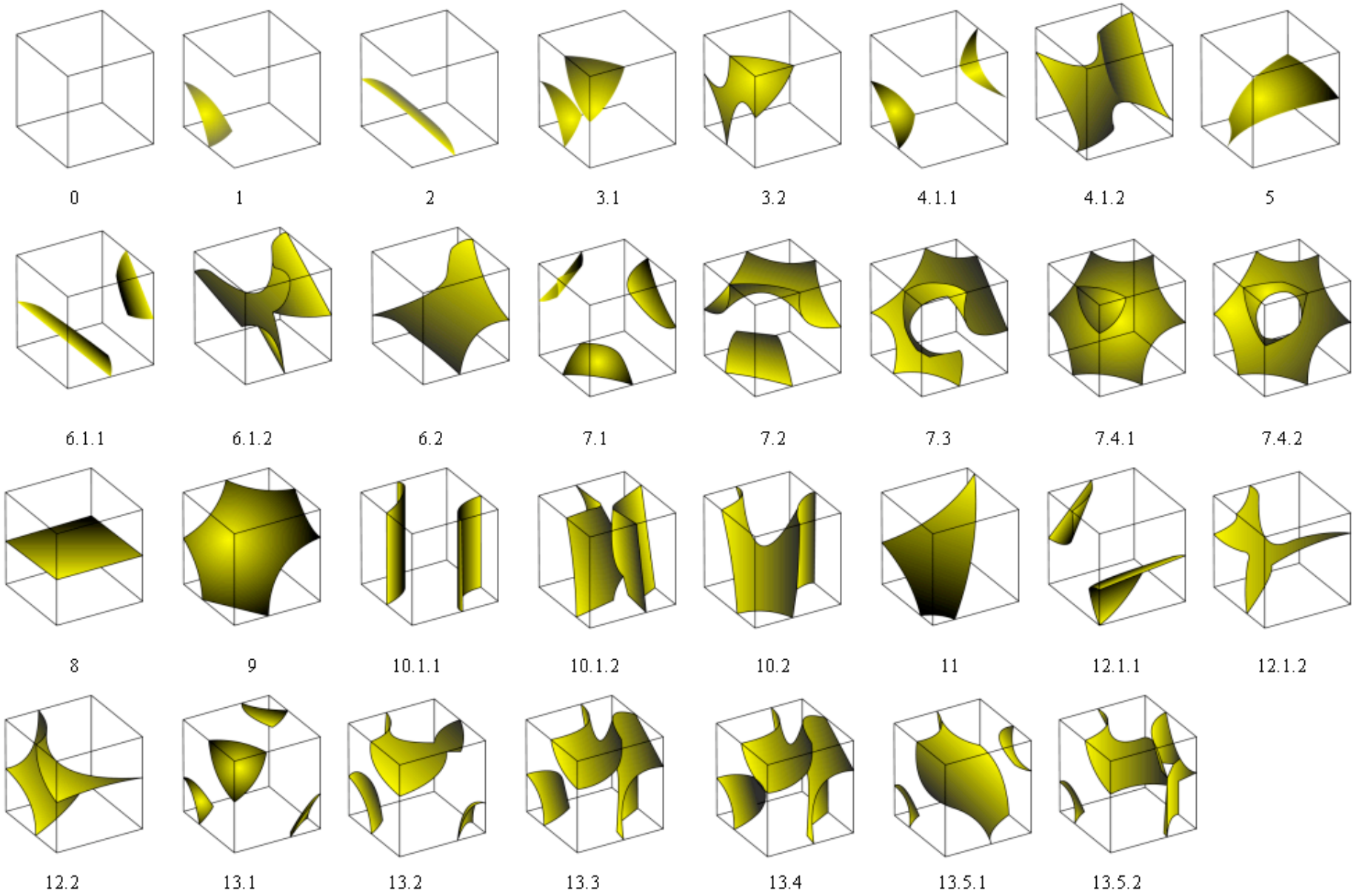

A-patches for Contouring Function Data
[Bajaj, et. Al 1994, 1995]

- Zero contour of a trivariate polynomial: f(x,y,z)=0
- Single-sheeted patches
- C^1 approximation of data within scaffold
- Conversion to Trimmed NURBS

Computing functions on surface

– Surface: Weighted least squares approximation of data points and signed-distance samples
– Function:Weighted least squares approximation of function values

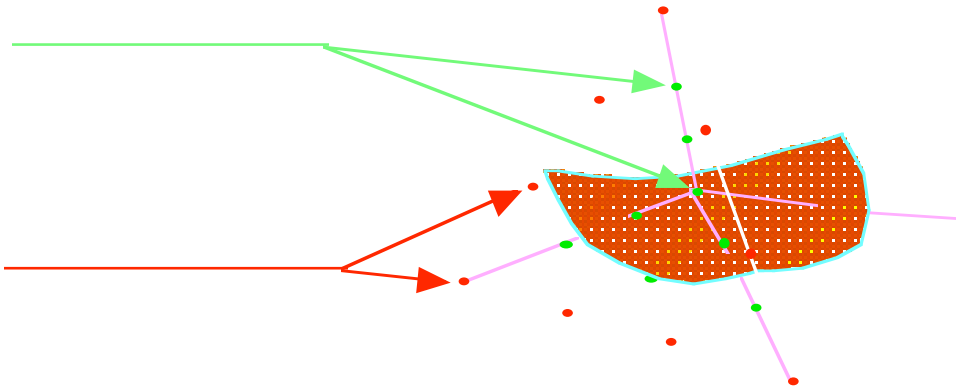

Tri/Tetra Meshing: Uniform 2D/3D Triangulation

Definitions:

Interior Edge in Boundary Cell - In a boundary cell, those edges with both vertices lying inside the volume are called interior edges.

Interior Face in Boundary Cell – in the boundary cell, those faces with all four vertices lying inside the volume are called interior faces.

Interior Cell - different from the boundary cell, all the eight vertices of an interior cell lie interior to the volume.

* Uniform 2D Triangulation

- Boundary intersection edge – blue triangles
- Interior edge in boundary cell – yellow triangles
- Interior cell – pink triangles

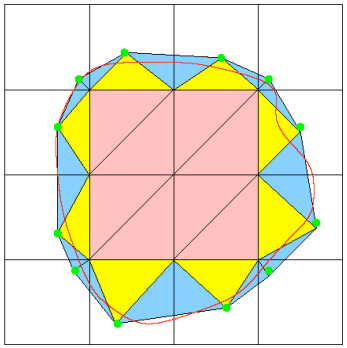

* Uniform 3D Tetrahedralization

- Boundary intersectione edge – blue tetras (a)
- Interior edge in boundary cell – yellow tetras (b&c)
- Interior face in boundary cell – (d,e&f)
- Interior cell (g&h)

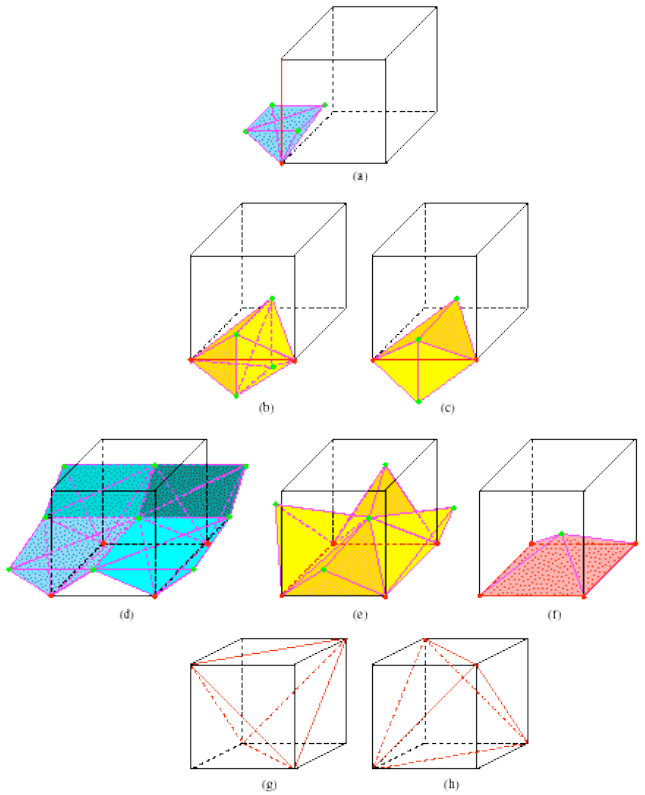

Case Table – uniform tetrahedralization

* Two isosurface components passing through the same cell – subdivide the cell

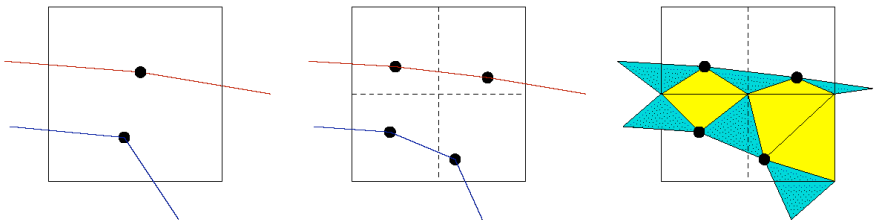

Center for Computational Visualization
Institute of Computational and Engineering Sciences
Department of Computer Sciences
University of Texas at Austin

Tri/Tetra Meshing: Hanging Node

Hanging Node - a hanging node is one that is attached to the corner of one triangle but does not attach to the corners of the adjacent triangles. Generally, a hanging node is a point that is a vertex for some elements (triangle, quad, tetra, hexa), but it is not for its other neighbor elements that share it. e.g., T-Vertex.

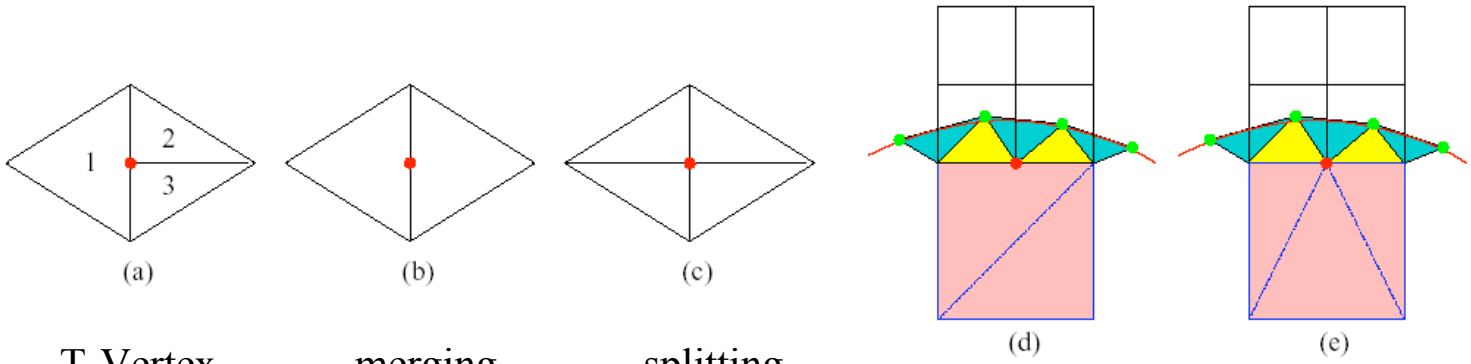

T-Vertex merging splitting Hanging node hanging node removal

Lemma: Only the interior cell needs to be modified if the splitting method is adopted.

Proof: the boundary cell and the interior cell

(1) Interior cell – since its neighbor cells may have higher resolution level, hanging nodes exist.

(2) Boundary cell – there are two rules for the sign change edge, the interior edge and the interior face.

- Minimal edge/face rule
- Only one minimizer is generated for each cell

Tri/Tetra Meshing: Adaptive 2D/3D Triangulation

* Adaptive 2D Triangulation

- Boundary Intersection edge – blue triangles
- Interior edge in boundary cell – yellow triangles
- Interior cell – pink triangles. In order to obtain triangles with good aspect ratio, we restrict the neighboring level different to be <= 2.

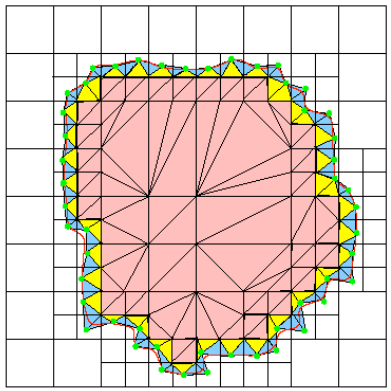

Adaptive Triangulation

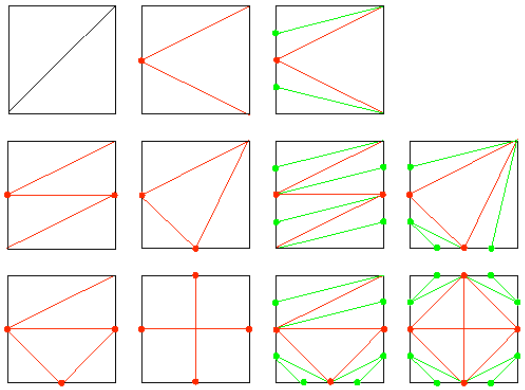

Case Table – interior cell (2D)

* Adaptive 3D Tetrahedralization

- Boundary intersectione edge – same.
- Interior edge in boundary cell – same.
- Interior face in boundary cell – same. The difference is to decompose it into triangles, each triangle and the minimizer construct a tetra.
- Interior cell – decompose each face into triangles, then construct tetras.

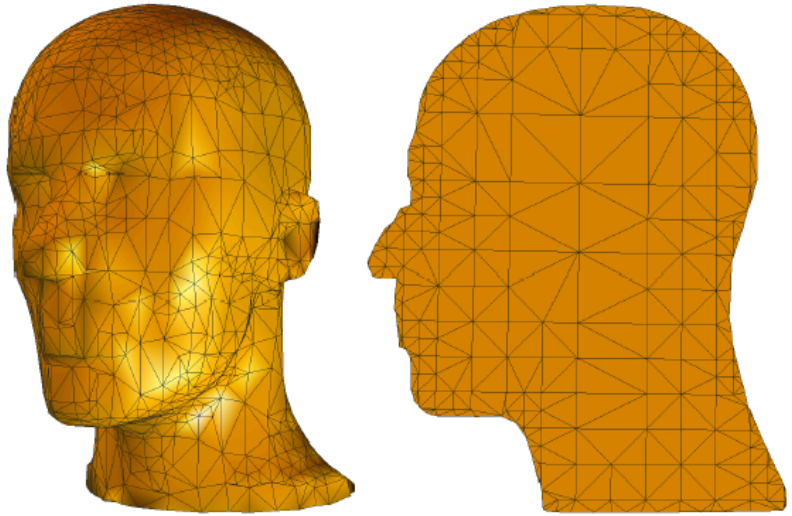

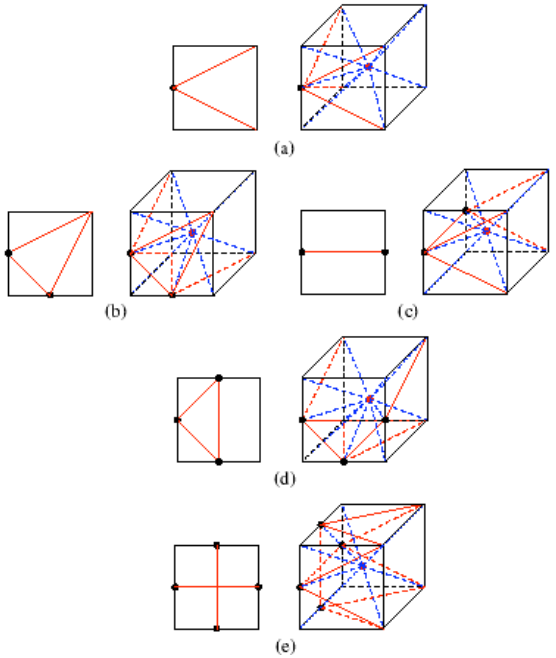

Case Table – interior cell (3D)

Center for Computational Visualization
Institute of Computational and Engineering Sciences
Department of Computer Sciences
University of Texas at Austin

Tri/Tetra Meshing: Topology and Error Function

Topology: Two dimensional example on recursive subdivision of a cubic cell in the finest level for reconstructing dual contour with correct topology.

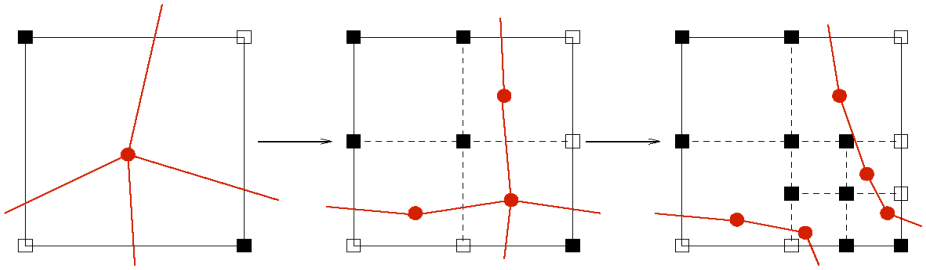

Non-manifold Non-manifold manifold

Feature Sensitive Error Metric:

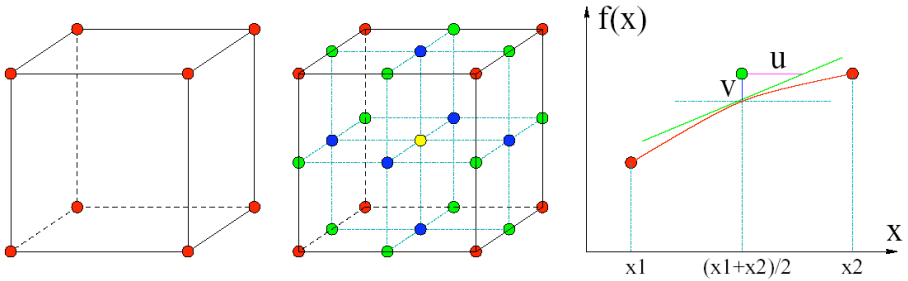

$$
\begin{aligned}
f^i(x,y,z) &= f_{000}(1-x)(1-y)(1-z) + f_{011}(1-x)yz \\
&+ f_{001}(1-x)(1-y)z + f_{101}x(1-y)z \\
&+ f_{010}(1-x)y(1-z) + f_{110}xy(1-z) \\
&+ f_{100}x(1-y)(1-z) + f_{111}xyz
\end{aligned}
$$

$$
error = \sum \frac{|f^{i+1} - f^i|}{|\nabla f^i|}
$$

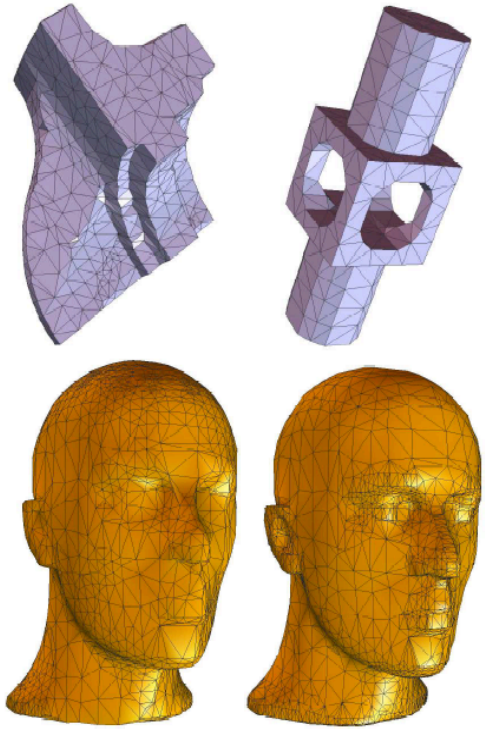

Upper row – sharp features; Bottom row – facial features, left: QEF (2952 tris), right: EDerror (2734 tris).

Center for Computational Visualization
Institute of Computational and Engineering Sciences
Department of Computer Sciences
University of Texas at Austin

Tri/Tetra Meshing: Results

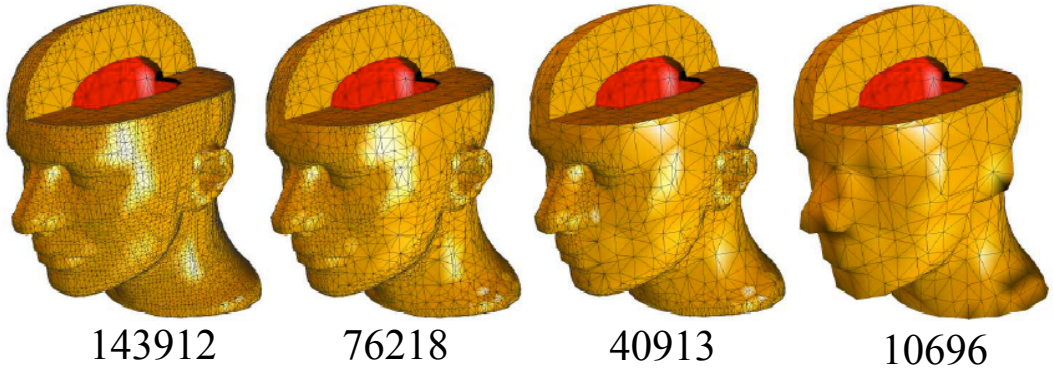

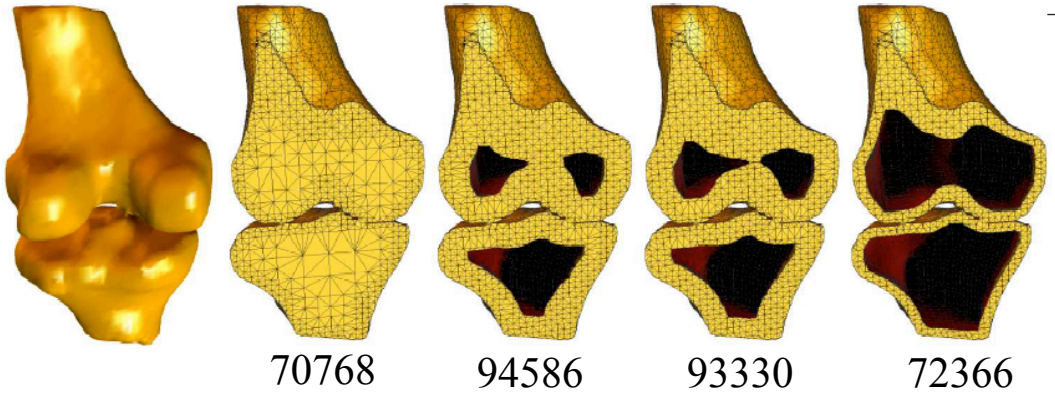

Dataset	Type	Size	Number of Tetrahedra (Extraction Time (unit : ms))			
			(a)	(b)	(c)	(d)
mAChE	Given	257^3	670642 (10891)	–	–	–
Heart	SDF	257^3	689020 (11110)	–	–	–
Skull	CT	129^3	715892 (12985)	579834 (10203)	365215 (7922)	166271 (3063)
Skin	CT	129^3	–	935124 (17406)	545269 (10468)	69351 (312)
Poly	CT	257^3	–	276388 (5640)	63325 (1672)	14204 (672)
Head	SDF	65^3	143912 (2547)	76218 (1391)	40913 (766)	10696 (203)
Knee	SDF	65^3	70768 (1360)	94586 (1782)	93330 (1750)	72366 (1406)

Tri/Tetra Quality Improvement:

- Local refinement/coarsening – inserting/deleting veritces
  - refinement: edge bisection (Rivara 1997, Bajaj 1996), point insertion and templates.
  - coarsening: edge contraction
- Local remeshing - face/edge swapping (Freitag 1997)
- Mesh smoothing - relocating vertices

Edge swapping

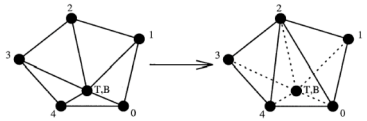

– Averaging methods
  - Laplacian smoothing (Field 1988): replace the node with the average of its neighbors.
  - Constrained/weighted Laplacian smoothing (Canann 1998, Bajaj 2002)

– Optimization-based methods (Canann 1998, Freitag 1995, 1997)
  - It measures the quality of the surrounding elements to a node, and attempt to optimize by computing the local gradient of the element quality w.r.t. the node location. The node moves along the increasing gradient direction until an optimum is reached.
  - Combined Laplacian/optimization-based approach

– Physically-based methods
  - Lohner (1986) simulates the force between neighboring nodes as a system of spring.
  - Shimada (1997) and Bossen (1996) view the nodes as the center of bubbles that are repositioned to attain equilibrium. Ansiostropic meshes can be achieved.

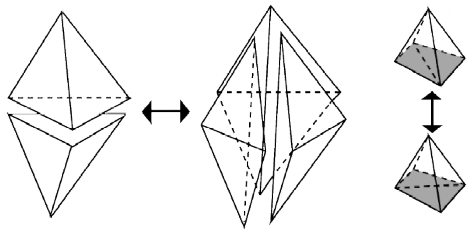

Face swapping

Tri/Tetra Quality Improvement: schemes

- Criteria:
  - Triangle: the aspect ratio = inscribed sphere radius / circumsphere radius
  - Tetrahedron:
    - Edge-ratio
    - Joe-Liu parameter
    - Minimum volume bound

$$F(s,d) = \frac{f(s,d)}{g(s,d)} = \frac{2^{2(1-\frac{1}{d})} \times 3^{\frac{d-1}{2}} \times |s|^{\frac{2}{d}}}{\sum_{0 \le i < j \le 3} |e_{ij}|^2}$$

- Edge contraction is used to reduce the worst edge-ratio.

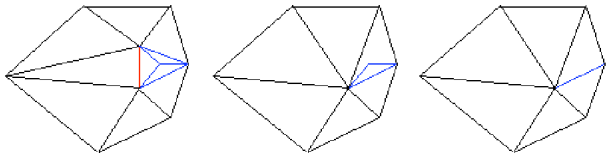

- Face/edge swapping

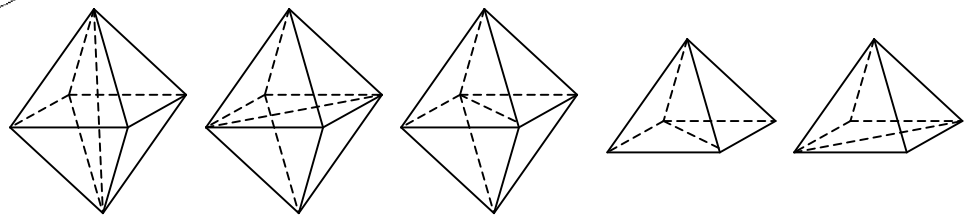

Diamond (interior edge) pyramid (sign change edge)

- Smoothing by relocating the node position
  - Interior node – use weighted averaging method (mass center)
  - boundary node – use various nonlinear geometric flows to improve the quality of the surface. The discretized formula of the Laplace-Beltrami operator is used.

Tri/Tetra Quality Improvement: Results

The edge-contraction and smoothing methods were implemented to improve the quality of tetra meshes.

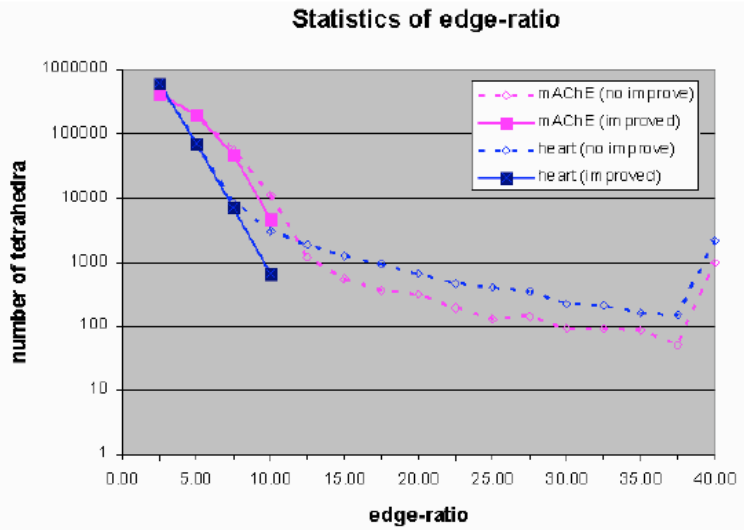

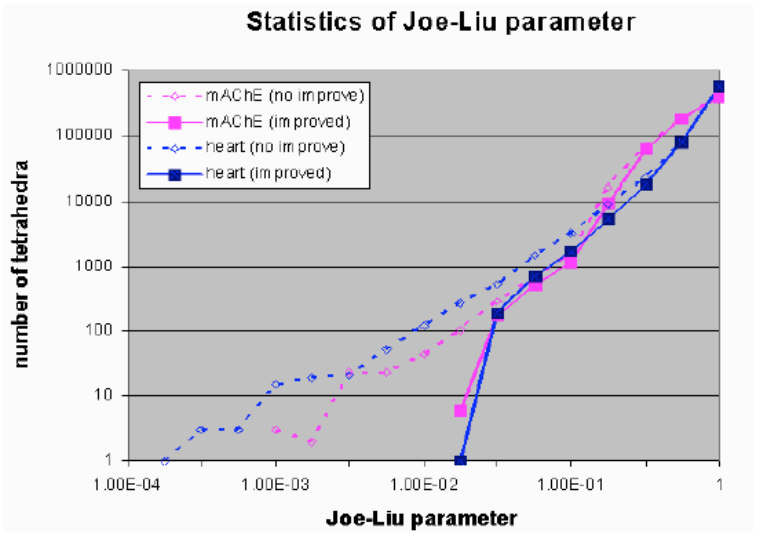

	Vertex Number	Tetra Number	Edge-ratio (best, worst)	Joe-Liu (best, worst)	Volume (minimal, maximal)
mAChE^b	124180	670642	$(1.03, 1.19\times10^{4})$	$(1.0, 6.24\times10^{-4})$	$(2.43\times10^{-7}, 9.40\times10^{6})$
mAChE^a	121670	656823	(1.03, 8.5)	$(1.0, 1.73\times10^{-2})$	$(1.40\times10^{-4}, 9.40\times10^{6})$
Heart^b	140425	689020	$(1.02, 1.20\times10^{5})$	$(1.0, 1.23\times10^{-4})$	$(4.88\times10^{-8}, 2.56\times10^{2})$
Heart^a	138072	676494	(1.02, 8.5)	$(1.0, 1.99\times10^{-2})$	$(4.39\times10^{-4}, 4.31\times10^{2})$

3. Quality Improvement with Geometric Flow

- Nonlinear geometric PDEs have been used to efficiently solve surface modeling problems: surface blending, N-sided filling and free-form surface fitting [1][2]. These nonlinear equations are discretized based on discrete differential geometry operators.

$$\frac{\partial x}{\partial t} = V_n(k_1, k_2, x)N(x), \quad M(0) = M_0.$$

Where $X(t)$ – a surface point on a closed surface $M(t)$

$Vn(k_1, K_2, x)$ – the normal velocity of $M(t)$

$N(x)$ – the unit normal of the surface at $x(t)$

- Mean Curvature Flow: $Vn = -H = -(k1 + k2)/2$
- Average Mean Curvature Flow: $Vn = h(t) - H(t)$

$$\text{where } h(t) = \int_{M(t)} H d\sigma / \int_{M(t)} d\sigma$$

- Surface Diffusion Flow: $V_n = \Delta H$
- High Order Flow: $\frac{\partial x}{\partial t} = (-1)^{k+1}\Delta^k H N(x)$

- Discretized Laplace-Beltrami operator over triangles [1][3]

$$\Delta f(p_i) = \frac{1}{A(p_i)} \sum_{j \in N_1(i)} \frac{\cot \alpha_{ij} + \cot \beta_{ij}}{2} [f(p_j) - f(p_i)],$$

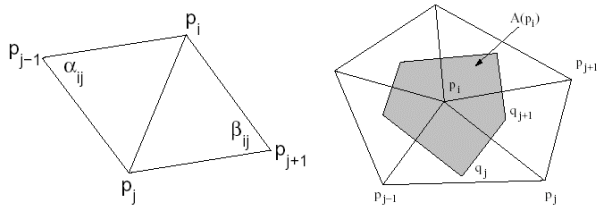

Fig 3.1: Left: The definition of the angles α_{ij} and β_{ij}. Right: The definition of the area $A(p_i)$.

$$H(p_i)N(p_i) = \frac{1}{2A(p_i)} \sum_{j \in N_1(i)} \frac{\cot \alpha_{ij} + \cot \beta_{ij}}{2} (p_i - p_j)$$

$$\Delta^k f(p_i) = \Delta(\Delta^{k-1} f)(p_i) = \frac{1}{A(p_i)} \sum_{j \in N_1(i)} \frac{\cot \alpha_{ij} + \cot \beta_{ij}}{2} [\Delta^{k-1} f(p_j) - \Delta^{k-1} f(p_i)]$$

References

1. Xu G., Pan Q., Bajaj C. **Discrete Surface Modeling using PDE's , CAGD, 2006**
2. Meyer M., Desbrun M., Schr*o*der P., Burr A. **Discrete Differential-Geometry Operators for Triangulated 2-Manifolds**. *VisMath'02,* 2002.

Quality Improvement with Geometric Flows

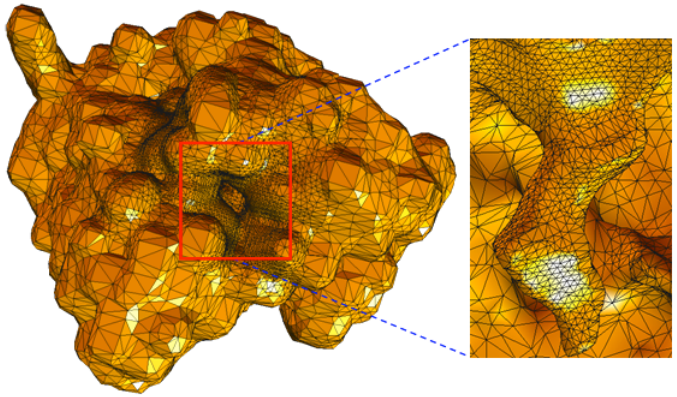

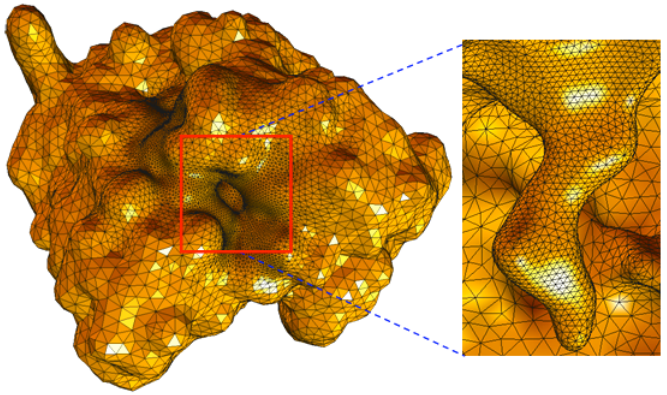

$$\frac{\partial x}{\partial t} = \Delta H(x)\vec{n}(x) + v(x)\vec{T}(x)$$

1. Denoising the surface mesh (vertex adjustment in the normal direction).
2. Improving the aspect ratio of the surface mesh (vertex adjustment in the tangent direction).
3. Improving the aspect ratio of the volumetric mesh (vertex adjustment inside the volume).

Properties:

1. Noise removal – normal movement
2. Feature preservation
   - Tangent movement doesn't change the shape
   - The surface diffusion flow is volume preserving
3. Quality improvement
4. Especially suitable for molecular meshes because the surface diffusion flow preserves sphere accurately if the initial mesh is close to a sphere.

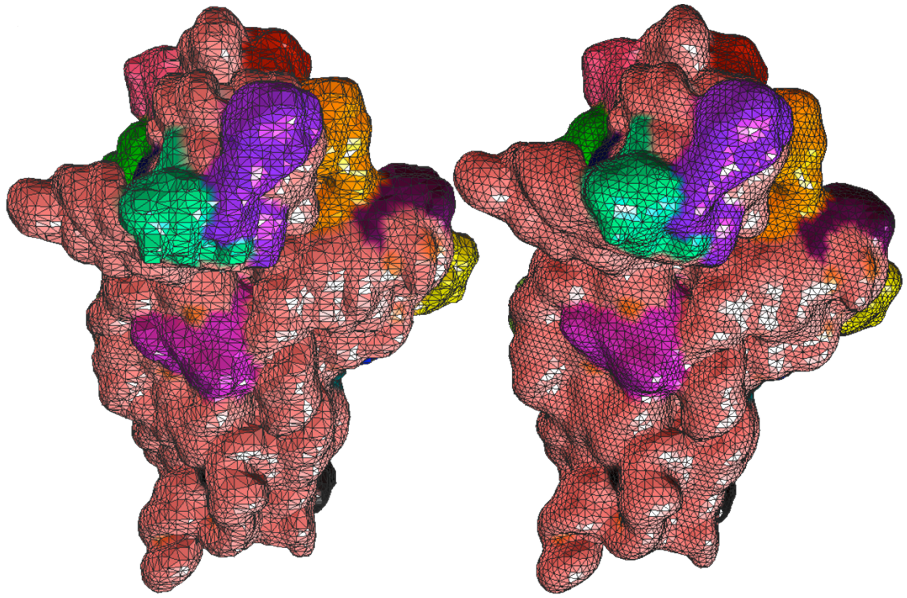

mAChE

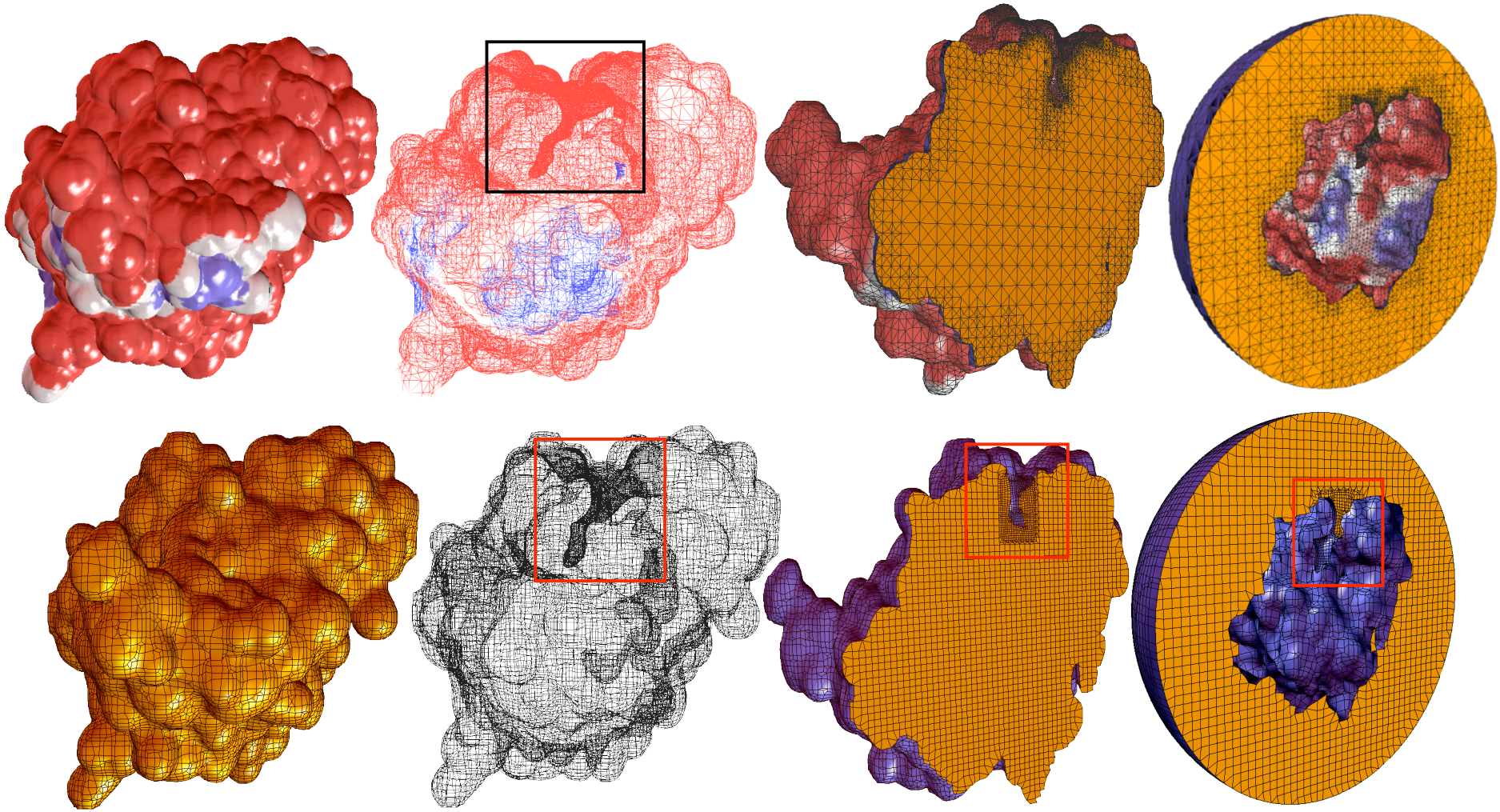

interior exterior

Center for Computational Visualization
Institute of Computational and Engineering Sciences
Department of Computer Sciences
University of Texas at Austin

Spline Heart Model

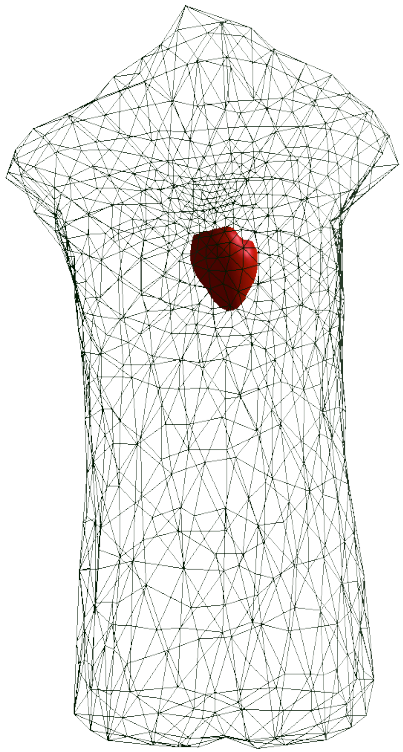

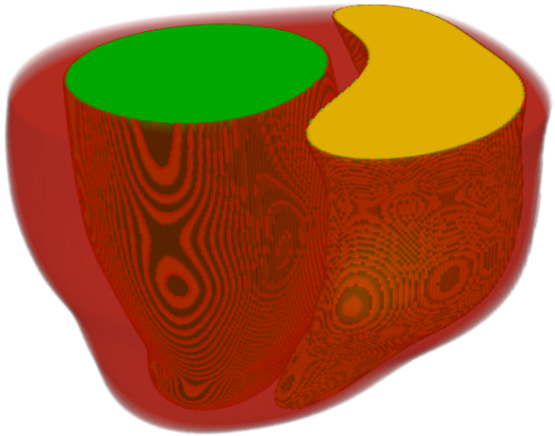

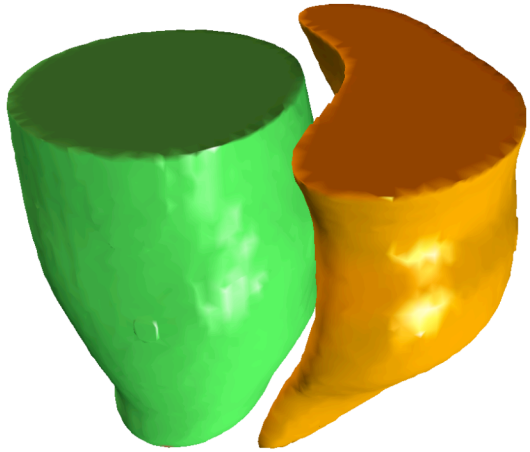

Center for Computational Visualization
Institute of Computational and Engineering Sciences
Department of Computer Sciences
University of Texas at Austin

Educational Heart Model

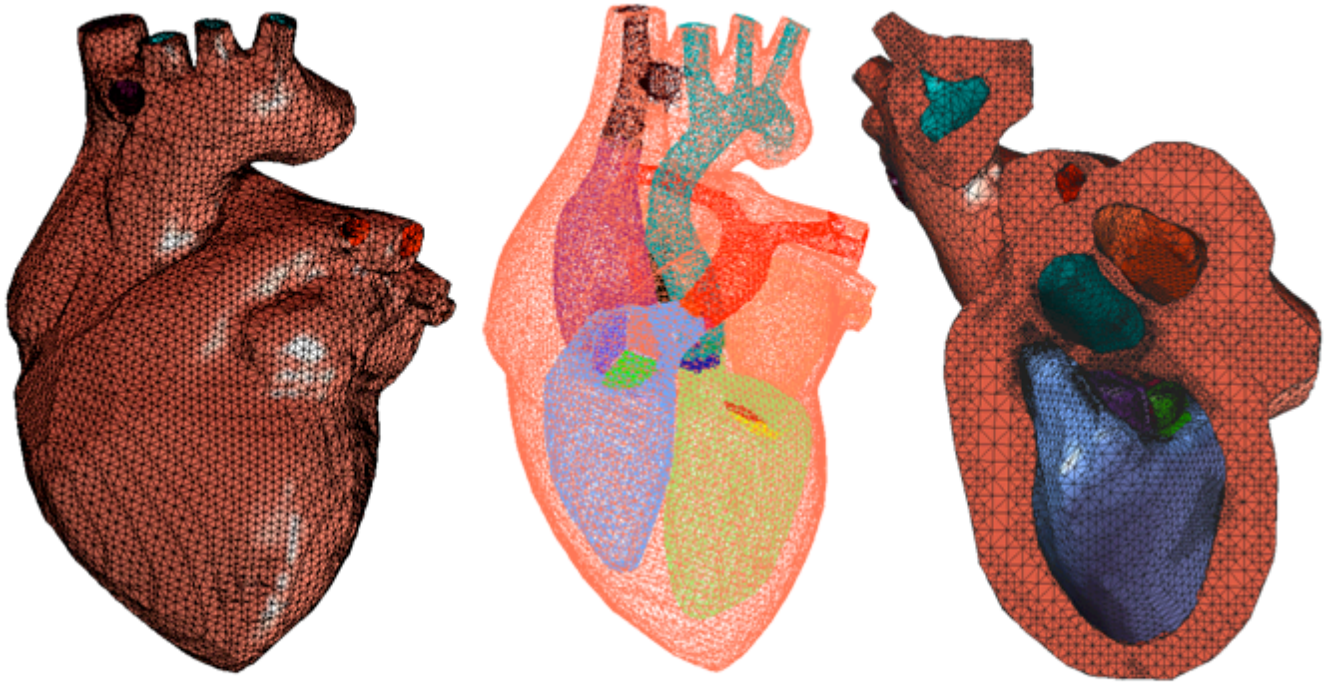

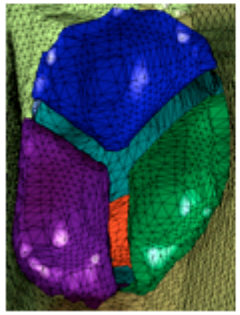

aortic valve

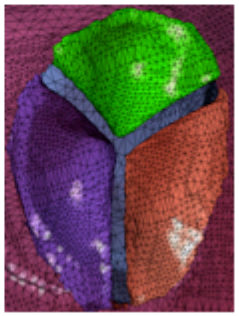

tricuspid valve

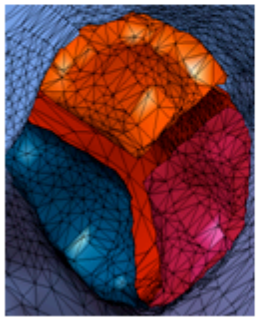

pulmonary valve

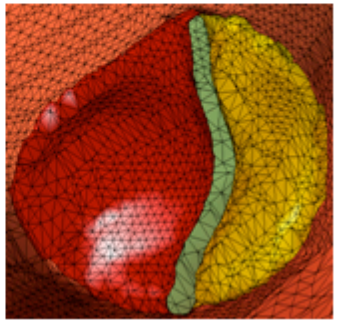

mitral valve

Center for Computational Visualization
Institute of Computational and Engineering Sciences
Department of Computer Sciences
University of Texas at Austin

Automatic CAD Model (features) Reconstruction from Point Clouds

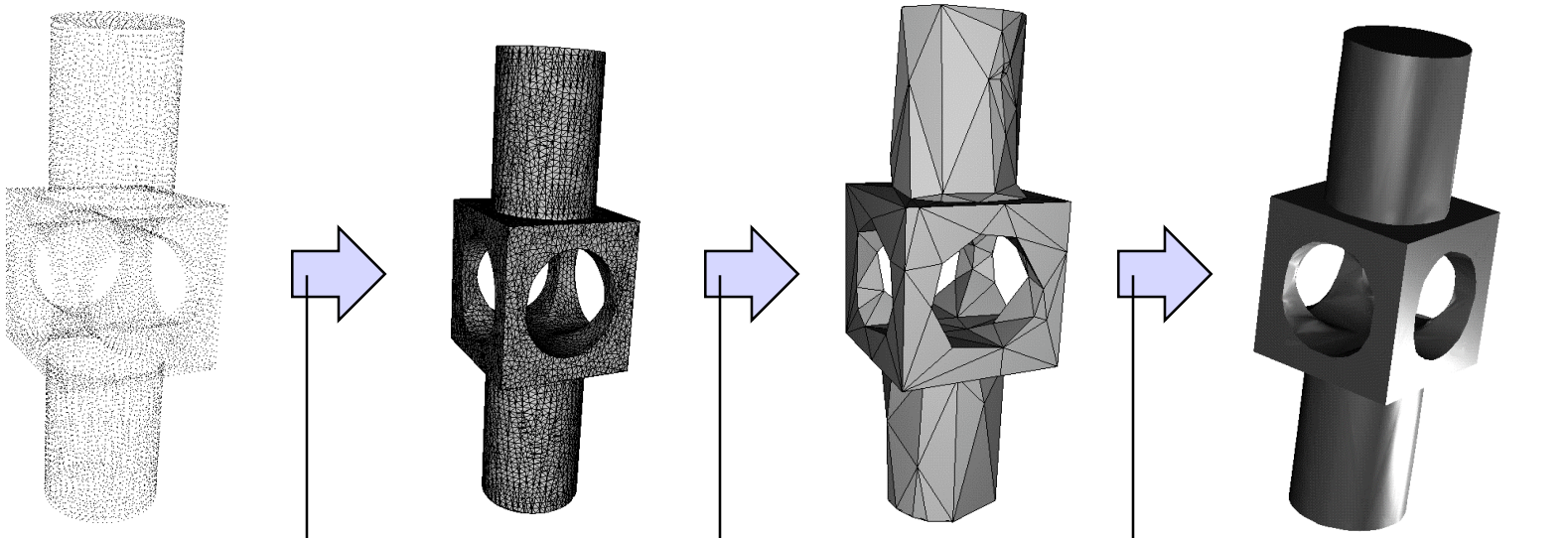

Sculpturing

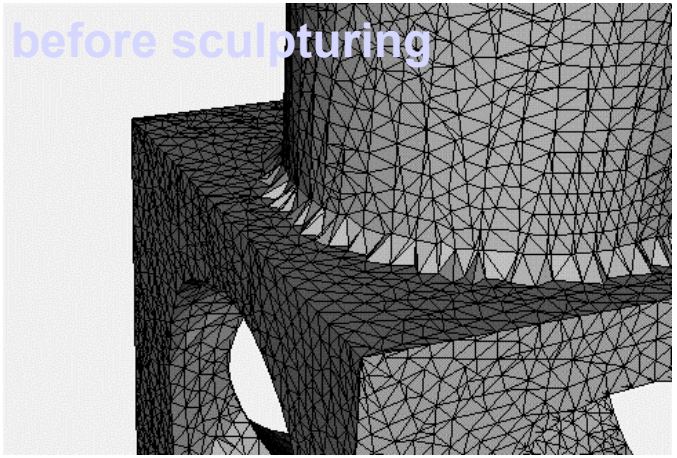

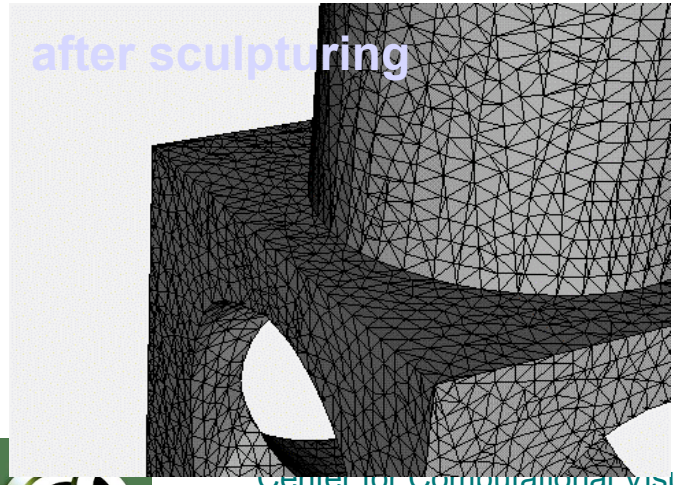

α -solid is refined by iteratively removing tetrahedra adjacent to the boundary, based on two principles:

– remove if a data point is occluded

– remove if sum of dihedral angles decreases

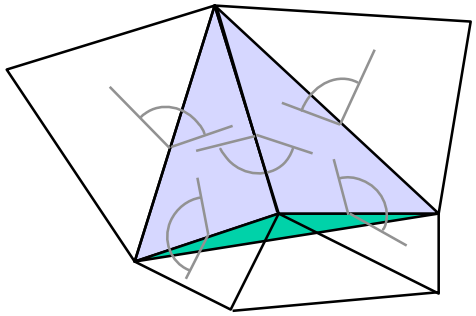

Dihedral angles formed by boundary faces

Mesh reduction

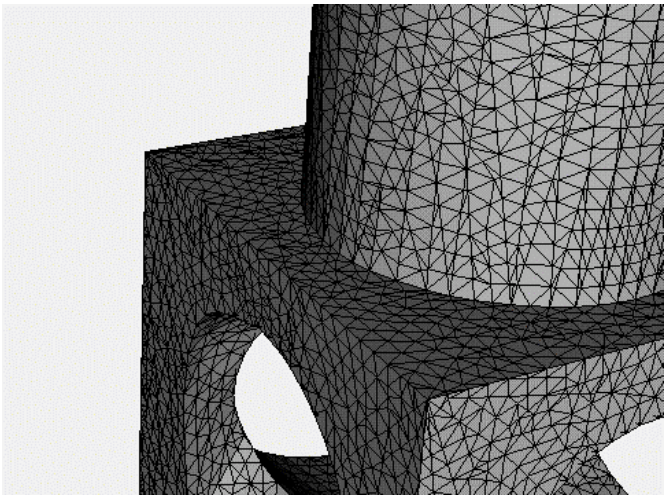

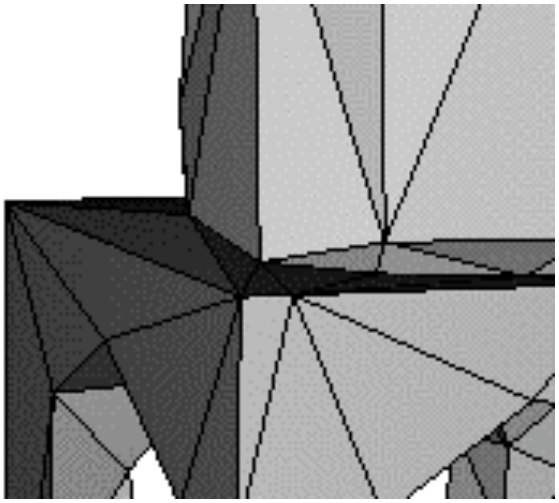

- *Mesh reduction technique for triangle meshes with multivariate data*

- Based on incremental deletion of vertices and retriangulation
- Guaranteed, global error-bound
- Sharp feature recognition and preservation

Surface Fitting

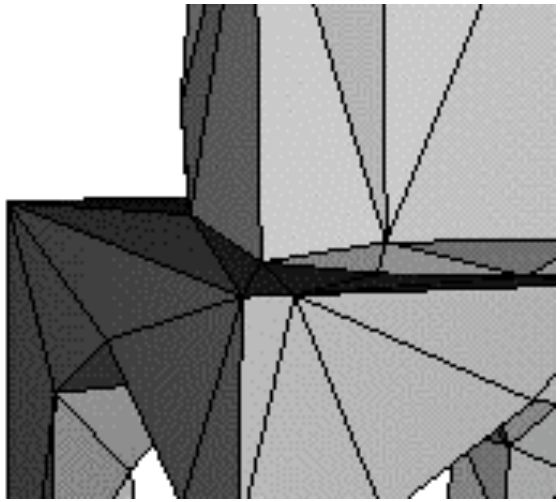

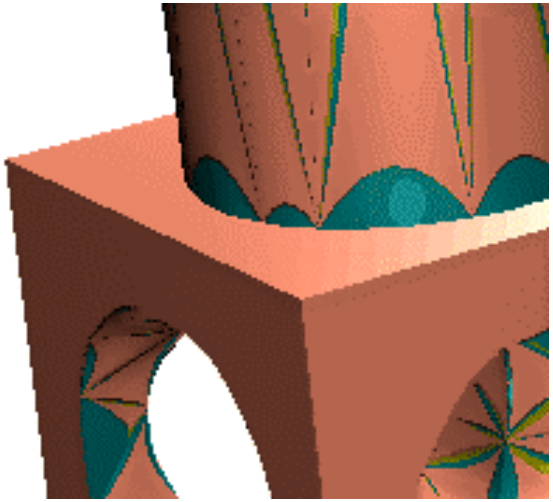

- Uses cubic A-patches (algebraic patches)
- C^1 continuity

- Sharp features (corners, sharp curved edges)
- Singularities

Further Reading

- **Introduction to Implicit Surfaces** *Morgan Kaufman Publishers Inc., (1997).*
- C. Bajaj, J. Chen, G. Xu **Modeling with Cubic A-patches** *ACM Transactions on Graphics, 14:2, (1995), 103-133.*
- C. Bajaj, F. Bernardini, G. Xu **Automatic Reconstruction of Surfaces and Scalar Fields from 3D Scans** *Proceedings: Computer Graphics (1995), Annual Conference Series, SIGGRAPH 95, ACM SIGGRAPH, 109-118***.**
- C. Bajaj **A Laguerre Voronoi Based Scheme for Meshing Particle Systems** *Japan Journal of Industrial and Applied Mathematics, (JJIAM), vol. 22, No. 2, Pages 167-177, June 2005*
- Y. Zhang, C. Bajaj. Adaptive and Quality Quadrilateral/Hexahedral Meshing from Volumetric Data. *Computer Methods in Applied Mechanics and Engineering (CMAME)*, 2005.
- Y. Zhang, C. Bajaj, B-S. Sohn. 3D Finite Element Meshing from Imaging Data. *The special issue of Computer Methods in Applied Mechanics and Engineering (CMAME) on Unstructured Mesh Generation*, 2004.
- Y. Zhang, G. Xu, C. Bajaj. Quality Meshing of Implicit Solvation Models of Biomolecular Structures. Computer Aided Geometric Design, 2006.